The mean tumor cellularity of urine sediments was 17.4% ($n = 7$, range 2.4–51.9%). Likewise, *FGFR3* mutations in exon 10 were detected in 5 of 13 (38.5%) tumor tissues of superficial bladder cancer and all cases harbored Y375C mutation. In analysis of urine sediments, Y375C mutation was detected in 4 of 5 cases (80%) harboring Y375C mutation in the primary tumor (Table 2). The mean tumor cellularity of mutation-positive cases was 63.1% ($n = 5$, range 6.5–100%) in tumor tissues and 35.1% ($n = 4$, range 2.1–100%) in urine sediments, respectively. No mutations were detected in exon 15 of *FGFR3* either in tissues or urine sediments (Table 2). In the analysis of muscle-invasive bladder cancer ($n = 6$) and 20 urine samples from patients with chronic cystitis, *FGFR3* mutations were not detected either in tumor tissues or urine sediments (data not shown).

Taken together, *FGFR3* mutations in superficial bladder cancer were detected in 12 of 13 (92.3%) tumor tissues and, in analysis of urine sediments, 11 (91.7%, except case no. 10) of 12 cases harboring mutations in primary tumor. One case (no. 1) showed multiple mutations comprising S249C in exon 7 and Y375C in exon 10 in tumor tissue, but only S249C in exon 7 was detected in the urine sample.

Discussion

The present study is the first report of the PNA-mediated real-time PCR clamping technique for detecting *FGFR3* mutation. The assay can be performed by a simple one-step reaction in a single tube using SYBR® green I fluorescent dye. PNA-mediated real-time PCR clamping screens for the presence or absence of mutations; however, PCR products can be easily subjected to direct sequencing to identify the type of mutation.

The amounts of genomic DNA extractable from urine sediments are often trace, particularly in patients during follow-up after TUR or with a small tumor burden; therefore, the method for detecting mutations should be sensitive and specific enough using a small amount of genomic DNA as the template. We validated that this assay enabled reproducible and reliable detection of mutations in a 100-fold excess amount of wild-type DNA using 50 ng of genomic DNA as the template, while it did not work well when the amount of template DNA was less than 10 ng due to the increase of assay CVs. In analysis using 1 ng of genomic DNA as the template, CPs of 1% or 10% standard was indistinguishable from that of 0% standard. CVs of CPs increased in reverse proportion to the decreasing amount of template DNA. In direct sequencing, all PCR products of 0% standard (wild type) amplified from 1 ng of template DNA showed mutations in PNA binding sites (Fig. 3C). Such mutations seemed to occur at random and this phenomenon may account for the increase of CVs of CPs in the experiment using a smaller amount of template DNA. In PCR, changes in the nucleotide sequence are attributable to errors made by DNA polymerase [13]. One nanogram of genomic DNA corresponds to 300 copies of genomic DNA and the length of the PCR product for exon 7 is 182 bps. Numbers of nucleotides in the target DNA are 5.46×10^4 and random errors will not interfere with subsequent analyses in conventional PCR, considering the fidelity (error rate per nucleotide) of *Taq* DNA polymerase is from $\sim 2 \times 10^{-4}$ to $< 1 \times 10^{-5}$ bps, however, PNA bound to wild-type sequences suppressed the amplification of template DNA. As a result, only part of the template DNA was available for PCR, and DNA fragments carrying misincorporated dNTPs would be amplified selectively. This phenomenon seems to be a limiting factor to define assay sensitivity in PNA-mediated real-time PCR clamping.

Thus, we optimized assay conditions to detect *FGFR3* mutations in exons 7, 10, and 15 in a 100-fold excess amount of wild-type DNA. In analysis using clinical samples, *FGFR3* mutations were detected in 92.3% (12/13) of superficial bladder cancer and no mutations were detected in muscle-invasive bladder cancer (0/6) or urine sediments of chronic cystitis (0/20). *FGFR3* mutations were detected in 91.7% (11/12) of urine sediments of which primary tumors presented *FGFR3* mutations. The types of mutations detected in urine sediments coincided with those of tumor tissues, except for one case (Case no. 1) with double mutations in exon 7 and exon 10, with urine sediments showing only a mutation in exon 7 of the FGFR3 gene. Our results suggested that this assay was highly sensitive and specific for detecting *FGFR3* mutations in urine samples.

Sensitive detection of *FGFR3* mutations in urine samples would be beneficial for monitoring tumor recurrence of superficial bladder cancer and would also be suitable as a favorable prognostic indicator in predicting the minimal risk of their progression to muscle-invasive bladder cancer. Further study is ongoing to elucidate the significance of *FGFR3* mutations detectable in urine samples in the clinical management of bladder UCC.

Acknowledgments

This work was supported in part by Grants-in-Aid for Cancer Research and by the Award of a Research Resident Fellowship from the Foundation for Promotion of Cancer Research (Japan) for the 3rd Term Comprehensive 10-Year Strategy for Cancer Control.

References

[1] American Cancer Society Cancer Facts and Figures 2005, American Cancer Society, Atalanta, 2005.
[2] K. Sugano, T. Kakizoe, Genetic alterations in bladder cancer and their clinical applications in molecular tumor staging, Nat. Clin. Pract. Urol. 3 (2006) 642–652.
[3] H.G. Wiener, C. Mian, A. Haitel, A. Pycha, G. Schatzl, M. Marberger, Can urine diagnostic tests replace cystoscopy in the management of bladder cancer? J. Urol. 159 (1998) 1876–1880.
[4] L. Prix, P. Uciechowski, B. Böckmann, M. Giesing, A.J. Schuetz, Diagnostic biochip array for fast and sensitive detection of K-ras mutations in stool, Clin. Chem. 48 (2002) 428–435.

[5] J.D. Luo, E.C. Chan, C.L. Shin, T.L. Chen, Y. Liang, T.L. Hwang, C.C. Chiou, Detection of rare mutant K-ras DNA in a single-tube reaction using peptide nucleic acid as both PCR clamp and sensor probe, Nucleic Acids Res. 34 (2006) e12.
[6] P.E. Nielsen, M. Egholm, R.H. Berg, O. Buchardt, Sequence-selective recognition of DNA by strand displacement with a thymine-substituted polyamide, Science 254 (1991) 1497–1500.
[7] L.H. Sobin, I.D. Fleming, TNM classification of Malignant Tumors, fifth edition (1997): Union Internationale Contre le Cancer and the American Joint Committee on Cancer, Cancer 80 (1997) 1803–1804.
[8] F.K. Mostofi, L.H. Sobin, H. Torloni, Histological Typing of Urinary Bladder Tumors: Intenational Classification of Tumors, No.10., World Health Organization, Switzerland, Geneva, 1973, pp. 21–31.
[9] M. Shigyo, K. Sugano, N. Fukayama, T. Taniguchi, K. Tobisu, H. Fujimoto, N. Doi, M. Niwakawa, K. Shimamura, T. Tsukamoto, Sekiya, T. Kakizoe, Allelic loss on chromosome 9 in bladder cancer tissues and urine samples detected by blunt-end single-strand DNA conformation polymorphism, Int. J. Cancer 78 (1998) 425–429.
[10] M. Liebert, G.A. Wedemeyer, J.A. Stein, R.W. Washington, A. Flint, L.Q. Ren, H.B. Grossman, Identification by monoclonal antibodies of an antigen shed by human bladder cancer cells, Cancer Res. 49 (1989) 6720–6726.
[11] I. Bernard-Pierrot, A. Brams, C. Dunois-Larde, A. Caillault, S.G. Diez de Medina, D. Cappellen, G. Graff, J.P. Thiery, D. Chopin, D. Ricol, F. Radvanyi, Oncogenic properties of the mutated forms of fibroblast growth factor receptor 3b, Carcinogenesis 27 (2006) 740–747.
[12] K. Sibley, D. Cuthbert-Heavens, M.A. Knowles, Loss of heterozygosity at 4p16.3 and mutation of FGFR3 in transitional cell carcinoma, Oncogene 20 (2001) 686–691.
[13] K.A. Eckert, T.A. Kunkel, DNA polymerase fidelity and the polymerase chain reaction, PCR Methods Appl. 1 (1991) 17–24.

Jpn J Clin Oncol 2007;37(12)907–912
doi:10.1093/jjco/hym139

Molecular Markers and Changes of Computed Tomography Appearance in Lung Adenocarcinoma with Ground-glass Opacity

Yukihiro Yoshida[1,4,7], Akiko Kokubu[1], Kenji Suzuki[4], Hidehiko Kuribayashi[2], Koji Tsuta[5], Yoshihiro Matsuno[5], Masahiko Kusumoto[6], Yae Kanai[3], Hisao Asamura[4], Setsuo Hirohashi[1,3] and Tatsuhiro Shibata[1,3]

[1]Cancer Genomics Project, [2]Proteome Bioinformatics Project and [3]Pathology Division, National Cancer Center Research Institute, 5-1-1, Tsukiji, Chuo-ku, Tokyo 104-0045, [4]Thoracic Surgery Division, [5]Clinical Laboratory Division and [6]Diagnostic Radiology Division, National Cancer Center Hospital, 5-1-1, Tsukiji, Chuo-ku, Tokyo 104-0045, Japan

Received March 31, 2007; accepted July 5, 2007; published online December 18, 2007

Background: High-resolution computed tomography (HRCT) of lung adenocarcinoma at early stage shows pure ground-glass opacity (GGO) and most cases of pure GGO remain stable during follow-up. There is no consensus on the strategy for follow-up. Identification of the molecular mechanisms that are associated with the natural history of lung adenocarcinoma should provide useful information.
Methods: Twenty-three lung adenocarcinomas that were followed-up for more than 6 months pre-operatively by HRCT were included in this study. Patterns of radiological changes during the follow-up period were classified into three groups; type 1, pure GGO without consolidation; type 2, appearance or increase in consolidation within pure GGO; type 3, consolidation without pure GGO. Mutational analysis of the epidermal growth factor receptor (EGFR) and K-ras genes and immunohistochemical staining of p53 protein were performed.
Results: EGFR mutations were found in 17 cases (74%), and there was no K-ras mutation. Positive staining of p53 was found in 8 cases (35%). As for radiological findings during the follow-up period, the frequencies of EGFR mutations and positive p53 staining were 67 and 0% in type 1 ($n = 9$), 89 and 44% in type 2 ($n = 9$) and 60 and 80% in type 3 ($n = 5$).
Conclusions: EGFR mutations were frequently found in lung adenocarcinoma with GGO on HRCT in this study. Inactivation of p53 may be associated with the appearance of central consolidation within pure GGO on HRCT which reflects invasive features and may be useful as a molecular marker during the follow-up of pure GGO.

Key words: lung neoplasms – tomography – spiral computed receptor – epidermal growth factor – tumor suppressor protein p53 – adenocarcinoma – bronchioloalveolar

INTRODUCTION

Due to recent advances in computed tomography (CT) imaging and the prevalence of lung cancer screening with the use of helical CT, the frequency of small and early lung cancers which are invisible on chest X-ray is increasing in Japan (1). Most pure ground-glass opacity (GGO) lesions detected by helical CT are stable in size during the follow-up period and are pathologically atypical adenomatous hyperplasia (AAH) or bronchioloalveolar carcinoma (BAC), which shows lepidic growth without invasion (2). Although the prognosis after surgical resection is excellent (2), some lesions with pure GGO progress rapidly (3). Although intensive and careful follow-up is required for pure GGO, it remains unknown how long and how often these should be followed.

A hypothesis of multistage carcinogenesis of lung adenocarcinoma was proposed, but it is still unclear how the lesion progresses over time in terms of radiological, pathological and molecular characteristics. Since it is technically and ethically difficult to obtain tissue samples from these lesions, most studies that have sought to reveal the natural history of lung adenocarcinoma were based on radiological findings during the pre-operative follow-up period (3–6). None of them examined the molecular

For reprints and all correspondence: Tatsuhiro Shibata, Cancer Genomics Project, National Cancer Center Research Institute, 5-1-1, Tsukiji, Chuo-ku, Tokyo 104-0045, Japan. E-mail: tashibat@ncc.go.jp

[7]Present address: Department of Thoracic Surgery, The University of Tokyo Hospital, Tokyo, Japan

markers that are associated with the natural history of lung adenocarcinoma.

Recently, somatic mutations of the epidermal growth factor receptor (EGFR) gene were reported in lung adenocarcinoma (7,8). They have also been found in AAH and BAC (9,10). Our previous study revealed that EGFR mutations occur in the early stage of lung adenocarcinoma, such as AAH and BAC, suggesting that they play an important role in disease progression, whereas AAH with K-ras mutations stays indolent (10). Consequently, we hypothesized that these two mutually exclusive mutations might determine the natural history of pure GGO lesions.

Identification of the molecular mechanisms that affect the biological behavior of GGO lesions may offer useful information for determining the appropriate follow-up strategy for pure GGO lesions. We examined the radiological changes and genetic aberrations for lesions that were followed-up preoperatively to clarify the molecular markers that are associated with the natural history of pure GGO.

PATIENTS AND METHODS

This is a retrospective cohort study. This study was approved by the institutional review board (date of IRB approval: 30 September 2005). First, we selected patients with more than 6 months interval between their first visit to the hospital and the date of the operation by using the National Cancer Center Hospital Thoracic Surgery Division Database, which is an electronic prospective database for surgical records. All charts of listed patients were reviewed to obtain further clinical and pathological information and to select appropriate cases that fulfilled all the following criteria: surgical cases from January 2000 to December 2004, pathological diagnosis of primary lung adenocarcinoma and cases that were followed-up for >6 months before the operation using high-resolution CT (HRCT). The aim of this study is to clarify the natural history of lung adenocarcinoma in view of radiological, pathological and molecular findings, so we excluded other potential etiologies for GGO such as AAH, infection, respiratory bronchiolitis which had been followed up for >6 months using HRCT and then surgically resected. We also excluded mucinous BAC and mucin-producing adenocarcinoma of the lung. Twenty-three cases were included in the study. Ten patients were followed up because of pure GGO lesion with its size of 15 mm or less, to which surgical resection would not be indicated until radiological changes such as increase in size or attenuation, appearance of consolidation were observed. Other reasons were diagnosis of inflammation on HRCT at the initial presentation ($n = 4$), the previous history of lung surgery in the contralateral side ($n = 4$), other malignancy under treatment ($n = 2$) and patient's request for further follow-up ($n = 3$). The median follow-up interval between the initial and last HRCT scan before the operation was 18 (6–62) months.

Radiological Diagnosis

CT was performed on helical or multidetector scanners (X-Vigor, TCT-900S units or Aquilion V-detector; Toshiba Medical Systems, Tokyo, Japan) as described previously (11,12). The helical technique in 14 examinations consisted of 10.0-mm collimation for individual scans of the entire lung [120 kV (peak), 150 mA] and reconstruction using a standard algorithm. Additional thin-section CT images at the level of the lesion were obtained using 2.0-mm collimation, a 20-cm field of view, 120 kVp and 200 mA per rotation, 1.0-s gantry rotation and a high spatial frequency reconstruction algorithm. The remaining 32 examinations were evaluated on a multidetector CT scanner using axial 2.0-mm × 4 modes (four images per gantry rotation), 120 kVp, 200 mA, and 0.5-s scanning time. Thin section CT images were obtained using 2.0-mm sections reconstructed at 2.0-mm intervals using a high spatial frequency algorithm and were retrospectively retargeted to each lung with a 20-cm field of view. In 17 examinations, nonionic iodinated contrast material was administered intravenously. The scans were viewed on standard mediastinal window setting (window level, 70 H; window width, 400 H) and lung window setting (window level, −600 H; window width, 1500–2000 H).

GGO and consolidation were defined based on our previous study (13). A GGO appearance on HRCT corresponds to lepidic growth of cancer cells along alveolar walls (BAC features), whereas the proportion of consolidation is a predictor of pathological invasiveness (13). Patterns of radiological changes during the follow-up period were classified into three types (Fig. 1): type 1, pure GGO without consolidation during the follow-up period; type 2, appearance or increase in consolidation within pure GGO during the follow-up period; type 3, consolidation without pure GGO during the follow-up period. A board-certified general thoracic surgeon who was unaware of clinical and experimental information (K.S.) diagnosed the findings.

A board-certified clinician who was unaware of clinical and experimental information (H.K.) encircled the lesion using the segmented line selection tool in Image J software and measured the largest diameter and perpendicular size of

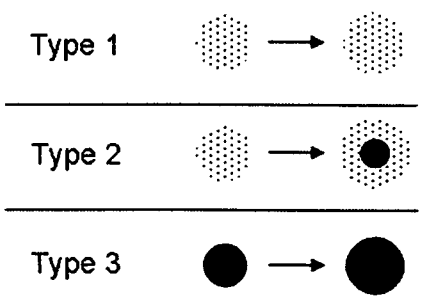

Figure 1. Schema of patterns of radiological changes during the follow-up period in this study.

the lesion (14). Corresponding slices in the initial and last HRCT examination were used. Tumor doubling time (TDT) was calculated using the formula proposed by Schwarts (15).

Mutational Analysis

Seven methanol-fixed and 16 formalin-fixed archives were used for mutational analysis of exons 18, 19 and 21 of the EGFR gene and exon 2 of the K-ras gene. Tumor DNA was purified by laser-captured microdissection (16). Information on primer sequences is available on request. Polymerase chain reactions and direct sequencing were performed as described previously (10). Peripheral lung tissue without cancer cells was used as a reference.

Pathological Diagnosis and Immunohistochemical Study

The pathological diagnosis of lung adenocarcinoma was categorized into four types according to the proposal by Ebright et al. (17): adenocarcinoma without BAC features, adenocarcinoma with BAC features (AwBF), BAC with focal invasion (BwFI) and pure BAC (PBAC).

Immunohistochemical staining of p53 was performed using a mouse primary antibody (1:100 dilution; clone DO7, Dako A/S, Glostrup, Denmark) and the avidin biotin complex method as described previously (18). A board-certified pathologist (K.T.) who was unaware of clinical and experimental information evaluated staining according to our previous criteria; +, when the proportion of tumor cells with definitely brownish nuclear staining was >20%; ±, when stained tumor cells were scattered, representing <20% of the tumor cells; −, when p53-positive cells were completely absent or seen only occasionally (19).

Clinical Information

Patient charts were reviewed to obtain clinical information. Patients who had quit smoking at least 1 year before the operation were defined as former smokers (20). Multiple lung cancers were discriminated from pulmonary metastases by applying the criteria proposed by Martini and Melamed (21). The TNM staging system revised in 1997 was adopted (22). All cases were cT1N0M0 and pT1N0M0. Surgical procedures were lobectomy in 11 cases, segmentectomy in 4 cases and wide wedge resection in 8 cases. The median follow-up period after the operation was 21 (9–65) months. Recurrence in the mediastinum was observed 12 months after the operation in one case with metachronous multiple lung cancers. The other 22 cases were alive without recurrence.

RESULTS

The 23 lesions are summarized in Table 1, and representative cases are shown in Figs. 2–5. Increase in size of 2 mm or more during follow-up period was observed in 10 cases (1 case was type 1, 5 were type 2 and 4 were type 3) and decrease in size of 2 mm or more was observed in one case of type 2 radiological classifications. The 8 men and 15 women had a median age of 66 years (37–77). Three were current smokers, 6 were former smokers and 14 were never smokers. There were seven cases of multiple lung cancers (metachronous in two cases and synchronous in five cases) and two cases were type 1, four were type 2 and 1one was type 3. Patients with type 3 radiological classification tended to have shorter interval between the initial and last HRCT examination and TDT of less than 24 months (Table 1).

EGFR mutations were found in 17 cases (74%), and all were somatic mutations (Table 2). There was no K-ras mutation in any of the 23 cases. Immunohistochemical staining of p53 was positive in eight cases (35%). Staining patterns were diffuse in all cases. Positive staining was

Table 1. Summary of clinical, pathological and radiological results

	Radiological findings		
	Type 1	Type 2	Type 3
Age, years			
Median	59	69	68
Range	40–75	53–77	37–74
Sex			
Female	7	6	2
Male	2	3	3
Smoking history			
Never	6	4	4
Former/current	3	5	1
Histological diagnosis			
PBAC	3	2	0
BwFI	6	7	3
AwBF	0	0	2
Size*, cm			
Median	1.4	1.6	1.6
Range	0.6–1.8	0.8–2.8	1.5–2.3
Interval**, months			
Median	20	16	12
Range	6–32	8–62	6–28
TDT			
0 < TDT < 24	3	3	4
24 < TDT	2	4	1
TDT < 0***	4	2	0

PBAC, pure bronchiolo-alveolar carcinoma; BwFI, BAC with focal invasion; AwBF, adenocarcinoma with BAC features; TDT, tumor doubling time; HRCT, high-resolution computed tomography.
*Size at the last HRCT examination.
**Interval between the initial and last HRCT examination.
***Reduction in volume during the follow-up period.

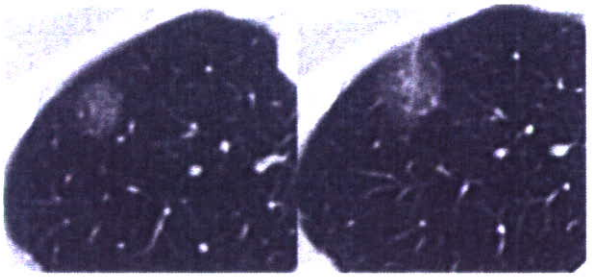

Figure 2. (Left: initial high-resolution computed tomography (HRCT); right: last HRCT; type 1 radiological finding) 66-year-old female, never smoker, 28-month interval; pure bronchioloalveolar carcinoma with del L747-T751.

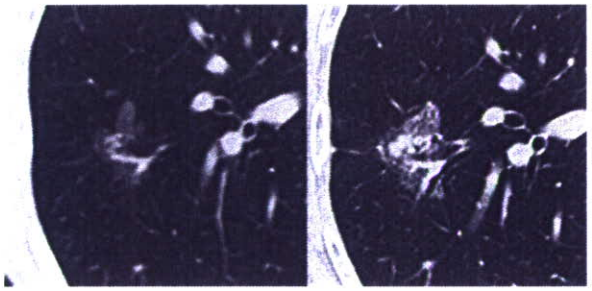

Figure 3. (Left: initial HRCT, right: last HRCT; type 2 radiological finding) 73-year-old female, never smoker, 11-month interval; BFWI with L858R.

observed both in the periphery of the lesion where cancer cells are lining along the alveolar walls and central areas where cancer cells are invading into the stroma.

The relationships between radiological findings, EGFR mutations and p53 staining are shown in Table 3. EGFR mutations were found in 67% of Type 1, 89% of Type 2 and 60% of Type 3. There was no trend between EGFR mutations and patterns of radiological changes during the follow-up period. The frequency of EGFR mutations was above 60% in all groups. The frequency of p53-positive was 44% in type 2 and 80% in type 3, in contrast to 0% in type 1. There was a trend between positive p53 immunohistochemistry and patterns of radiological changes during the follow-up period.

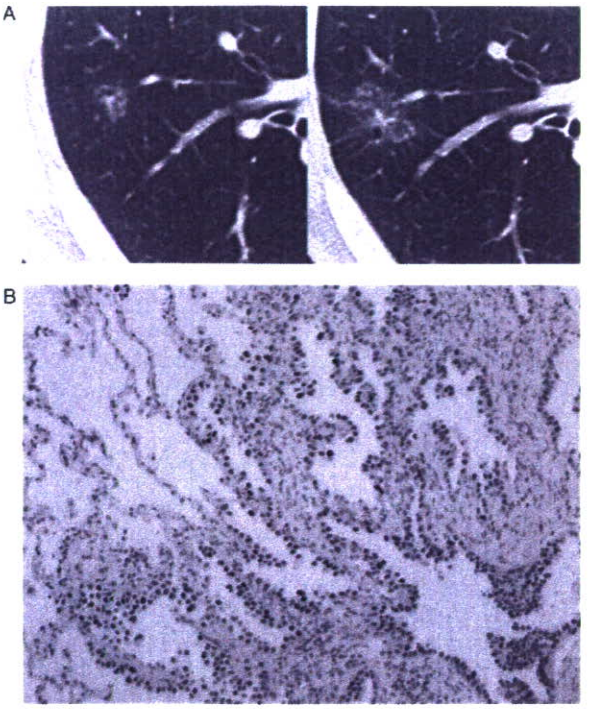

Figure 4. (A) (left: initial HRCT; right: last HRCT; type 2 radiological finding) 59-year-old male, former smoker, 62-month interval; BAC with focal invasion with del E746-A 750. (B) Immunohistochemical staining of p53 in the same case as in (A). p53 immunohistochemical staining showed reactivity in most tumor nuclei, but not in normal alveolar cells (hematoxylin and eosin staining, original magnification ×100).

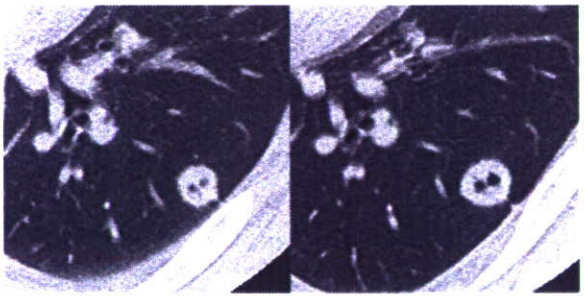

Figure 5. (Left: initial HRCT; right: last HRCT; type 3 radiological finding) 37-year-old male, never smoker, 6-month interval; adenocarcinoma with BAC features with wild type.

DISCUSSION

Several studies have been conducted to reveal the natural history of lung adenocarcinoma based on radiological findings during the pre-operative follow-up period (3–6). Most of them were based on the screening with low-dose CT, conventional CT with a 10 mm interval, which was not appropriate for a detailed and precise analysis of radiological findings. No study has ever examined molecular markers. To clarify the natural history of lung adenocarcinoma in view of radiological, pathological and molecular findings, we examined selected cases of patients who were followed-up for at least 6 months using HRCT pre-operatively and investigated the molecular markers that may be associated with the pattern of radiological changes during the follow-up period.

Biological behaviors of pure GGO may be determined by either initial aberrations of multistage carcinogenesis or additional aberrations during its progression. Since we

Table 2. EGFR mutations detected in the present study

Exons	Amino acids	Nucleotides	No. of patients
Exon 19	del E746-A750	del 2235-2249	1
	del E746-A750	del 2236-2250	6
	del E746-T751insS	del2236-2251 + insT	1
	del L747-T751	del 2239-2253	3
Exon 21	L858R	Substitution of G for T at nucleotide 2573	6

EGFR, epidermal growth factor receptor.

Table 3. EGFR mutations, immunohistochemical staining of p53 and patterns of radiological changes during the follow-up period

	Number	EGFR mutation	Deletions in Exon 19	L858R	Positive p53 IHC
Type 1	9	67%	4	2	0%
Type 2	9	89%	5	3	44%
Type 3	5	60%	2	1	80%

IHC, immunohistochemistry.

previously demonstrated that both EGFR and K-ras mutations were early events in lung adenocarcinoma (10), we examined whether these mutations were associated with the natural history of pure GGO.

We detected EGFR mutations in 17 cases (74%). Such a high incidence of EGFR mutations was probably due to the fact that all of the lesions in our study were AwBF, which frequently harbor EGFR mutations (20). We consistently observed EGFR mutations in most of the lesions with a GGO appearance (78% in types 1 and 2).

We classified lung adenocarcinoma in terms of the pattern of radiological changes during the follow-up period into three types and investigated differences between them from a molecular perspective. In our study, we should consider that the patterns of radiological changes during the follow-up period may not be distinct from each other, but rather they might be a transient finding in multistage carcinogenesis of lung adenocarcinoma. Lesions with a type 1 radiological classification might progress to type 2 and eventually type 3 during a long follow-up. The frequent EGFR mutations in type 1 (67%) suggested that they play a role in initiation (Table 3). However, EGFR mutations failed to distinguish the radiological classifications from each other, in contrast to our hypothesis, and this suggested that such mutations have little association with the progressive behavior of pure GGO.

There was no case of positive p53 staining in type 1 in our study, in contrast to type 2 (44%) and type 3 (80%). Our result suggests that the inactivation of p53 might be associated with the appearance of consolidation within a pure GGO lesion on HRCT which reflects invasive features of the lesion. Therefore, p53 should be a useful biomarker for determining the follow-up strategy for pure GGO lesions. The detection of serum p53 auto-antibodies, e.g. might complement a radiological follow-up, prevent the unnecessary exposure to X-rays and even precede HRCT findings to determine the appropriate timing for surgical intervention without delay (23,24). Previous study by others also demonstrated that among lung AwBF, the frequency of positive p53 staining was low in PBAC, whereas it increased in accordance with invasive features and they concluded that p53 played an important role in the progression of lung adenocarcinoma, although their study did not take into account periodic changes (19).

Since lung nodules that are stable for 2 years are considered to be benign, we defined a TDT cut-off value of 2 years in Table 1 (25). However, we have to be careful when applying TDT to lesions with GGO, in which cancer cells grow in a lepidic fashion without filling alveolar spaces. In addition, some lung adenocarcinomas retract the surrounding structures and shrink in size during their progression, which makes it difficult to interpret TDT (3).

Our study has several limitations, such as the small number of patients, the short follow-up between the initial and last HRCT examination and possible inter-observer variability of HRCT findings. Furthermore, the results may have been biased since we only considered surgically resected cases and we have no data on genetic aberrations for pure GGO that is stable and followed-up without surgical resection. Although K-ras mutations are frequently found in mucinous BAC or mucin-producing adenocarcinoma of the lung (26), we found no K-ras mutation in this study. The progression of multistage carcinogenesis in lung adenocarcinoma with K-ras mutations remains unclear.

It is important that we understand multistage carcinogenesis of lung adenocarcinoma to identify molecular biomarkers which can discriminate pure GGO lesions which progress from those which stay indolent. We found that the inactivation of p53 might be associated with the appearance of central consolidation within pure GGO on HRCT in this study. These markers should offer useful information for determining the appropriate strategy regarding the interval and duration of follow-up for pure GGO lesions detected by helical CT.

FUNDING

This work was supported in part by Public Trust Haraguchi Memorial Cancer Research Fund, a grant-in-aid for the Comprehensive 10-Year-Strategy for Cancer Control from the Ministry of Health, Labor and Welfare, Japan and the Program for Promotion of Fundamental Studies in Health Sciences of the National Institute of Biomedical Innovation (NiBio), Japan.

Conflict of interest statement

None declared.

References

1. Kaneko M, Eguchi K, Ohmatsu H, Kakinuma R, Naruke T, Suemasu K, et al. Peripheral lung cancer: screening and detection with low-dose spiral CT versus radiography. *Radiology* 1996;201:798–802.
2. Nakata M, Sawada S, Saeki H, Takashima S, Mogami H, Teramoto N, et al. Prospective study of thoracoscopic limited resection for ground-glass opacity selected by computed tomography. *Ann Thorac Surg* 2003;75:1601–5.
3. Kakinuma R, Ohmatsu H, Kaneko M, Kusumoto M, Yoshida J, Nagai K, et al. Progression of focal pure ground-glass opacity detected by low-dose helical computed tomography screening for lung cancer. *J Comput Assist Tomogr* 2004;28:17–23.
4. Aoki T, Nakata H, Watanabe H, Nakamura K, Kasai T, Hashimoto H, et al. Evolution of peripheral lung adenocarcinomas: CT findings correlated with histology and tumor doubling time. *AJR Am J Roentgenol* 2000;174:763–8.
5. Kodama K, Higashiyama M, Yokouchi H, Takami K, Kuriyama K, Kusunoki Y, et al. Natural history of pure ground-glass opacity after long-term follow-up of more than 2 years. *Ann Thorac Surg* 2002;73:386–92.
6. Takashima S, Maruyama Y, Hasegawa M, Yamanda T, Honda T, Kadoya M, et al. CT findings and progression of small peripheral lung neoplasms having a replacement growth pattern. *AJR Am J Roentgenol* 2003;180:817–26.
7. Lynch TJ, Bell DW, Sordella R, Gurubhagavatula S, Okimoto RA, Brannigan BW, et al. Activating mutations in the epidermal growth factor receptor underlying responsiveness of non-small-cell lung cancer to gefitinib. *N Engl J Med* 2004;350:2129–39.
8. Paez JG, Janne PA, Lee JC, Tracy S, Greulich H, Gabriel S, et al. EGFR mutations in lung cancer: correlation with clinical response to gefitinib therapy. *Science* 2004;304:1497–500.
9. Yatabe Y, Kosaka T, Takahashi T, Mitsudomi T. EGFR mutation is specific for terminal respiratory unit type adenocarcinoma. *Am J Surg Pathol* 2005;29:633–9.
10. Yoshida Y, Shibata T, Kokubu A, Tsuta K, Matsuno Y, Kanai Y, et al. Mutations of the epidermal growth factor receptor gene in atypical adenomatous hyperplasia and bronchioloalveolar carcinoma of the lung. *Lung Cancer* 2005;50:1–8.
11. Oshiro Y, Kusumoto M, Matsuno Y, Asamura H, Tsuchiya R, Terasaki H, et al. CT findings of surgically resected large cell neuroendocrine carcinoma of the lung in 38 patients. *AJR Am J Roentgenol* 2004;182:87–91.
12. Tateishi U, Muller NL, Johkoh T, Maeshima A, Asamura H, Satake M, et al. Mucin-producing adenocarcinoma of the lung: thin-section computed tomography findings in 48 patients and their effect on prognosis. *J Comput Assist Tomogr* 2005;29:361–8.
13. Asamura H, Suzuki K, Watanabe S, Matsuno Y, Maeshima A, Tsuchiya R. A clinicopathological study of resected subcentimeter lung cancers: a favorable prognosis for ground glass opacity lesions. *Ann Thorac Surg* 2003;76:1016–22.
14. Abramoff MD, Magelhaes PJ, Ram SJ. Image Processing with Image J. *Biophotonics International* 2004;11:36–42.
15. Schwarts M. A biomathematical approach to clinical tumor growth. *Cancer* 1961;14:1272–94.
16. Emmert-Buck MR, Bonner RF, Smith PD, Chuaqui RF, Zhuang Z, Goldstein SR, et al. Laser capture microdissection. *Science* 1996;274:998–1001.
17. Ebright MI, Zakowski MF, Martin J, Venkatraman ES, Miller VA, Bains MS, et al. Clinical pattern and pathologic stage but not histologic features predict outcome for bronchioloalveolar carcinoma. *Ann Thorac Surg* 2002;74:1640–6.
18. Etoh T, Kanai Y, Ushijima S, Nakagawa T, Nakanishi Y, Sasako M, et al. Increased DNA methyltransferase 1 (DNMT1) protein expression correlates significantly with poorer tumor differentiation and frequent DNA hypermethylation of multiple CpG islands in gastric cancers. *Am J Pathol* 2004;164:689–99.
19. Terasaki H, Niki T, Matsuno Y, Yamada T, Maeshima A, Asamura H, et al. Lung adenocarcinoma with mixed bronchioloalveolar and invasive components: clinicopathological features, subclassification by extent of invasive foci, and immunohistochemical characterization. *Am J Surg Pathol* 2003;27:937–51.
20. Takano T, Ohe Y, Sakamoto H, Tsuta K, Matsuno Y, Tateishi U, et al. Epidermal growth factor receptor gene mutations and increased copy numbers predict gefitinib sensitivity in patients with recurrent non-small-cell lung cancer. *J Clin Oncol* 2005;23:6829–37.
21. Martini N, Melamed MR. Multiple primary lung cancers. *J Thorac Cardiovasc Surg* 1975;70:606–12.
22. Mountain CF. Revisions in the international system for staging lung cancer. *Chest* 1997;111:1710–7.
23. Lubin R, Zalcman G, Bouchet L, Tredanel J, Legros Y, Cazals D, et al. Serum pp53 antibodies as early markers of lung cancer. *Nat Med* 1995;1:701–2.
24. Mitsudomi T, Suzuki S, Yatabe Y, Nishio M, Kuwabara M, Gotoh K, et al. Clinical implications of p53 autoantibodies in the sera of patients with non-small-cell lung cancer. *J Natl Cancer Inst* 1998;90:1563–8.
25. MacMahon H, Austin JH, Gamsu G, Herold CJ, Jett JR, Naidich DP, et al. Fleischner Society; Guidelines for management of small pulmonary nodules detected on CT scans: a statement from the Fleischner Society. *Radiology* 2005;237:395–400.
26. Kobayashi T, Tsuda H, Noguchi M, Hirohashi S, Shimosato Y, Goya T, et al. Association of point mutation in c-Ki-ras oncogene in lung adenocarcinoma with particular reference to cytologic subtypes. *Cancer* 1990;66:289–94.